Quantitative Investigation of the Morphologically Corrugated CVD-grown Graphene Monolayer Surface with a Nanoparticle-on-Mirror system

Won-Hwa Park (s952151@gmail.com)
Inha University https://orcid.org/0000-0002-8629-6185

Research Article

Keywords: Graphene Monolayer, Chemical Vapor Deposition, Plasmonics, Nanoparticle-on-Mirror, Radial Breathing-Like Mode, Bio-sensing

Posted Date: January 12th, 2022

DOI: https://doi.org/10.21203/rs.3.rs-1206534/v1

Version of Record: A version of this preprint was published at Plasmonics on April 5th, 2022. See the published version at https://doi.org/10.1007/s11468-022-01634-7.

Abstract

Graphene can be used as a starting material for the synthesis of useful nano-complexes for flexible, transparent electrodes, therapeutic, bio-diagnostics and bio-sensing. In order to apply graphene in the medical field, chemical vapor deposition (CVD) method has been mainly utilized considering its large and near-homogenious carbon constituents. Especially, the less degree of perturbation of graphene monolayer (GM), which is followed by the underneath catalytic Cu surface morphology, is very crucial in terms of providing the suspended GM and relatively fluent lateral carrier mobility with lower sheet resistance value. In this work, we can suggest a surface-Enhanced Raman Spectroscopic (SERS) indicator in a quantitative way on the status of z-directional morphological corrugation of a CVD–grown GM (CVD-GM) by applying a Nanoparticle-on-Mirror (NPoM) system composed of Au nanoparticle (NP) / CVD-GM / Au thin film (TF) plasmonic junction structure. A new (or enhanced) Radial Breathing Like Mode (RBLM) SERS signal around ~150 cm^{-1} from CVD-GM spaced in NPoM is clearly observed by employing a local z-polarized incident field formed at the Au NP–Au TF plasmonic gap junctions.

With this observation, the value of I[out-of-plane, RBLM] / I[in-plane, [2D] at certain domains, it can be suggested as a new optical nano-metrology value to relatively determine between lower z-directional morphological corrugation (or protrusion) status of a CVD-GM spaced in our NPoM system (lower I[RBLM] / I[2D] value) and higher degree of lateral carrier mobility of the CVD-GM associated with lower sheet resistance values as a result of higher blue-shifted Raman in-plane (G, 2D) peak maximum position. Furthermore, we will also expect the bio-sensing performances by utilizing the high specific surface area and ultrahigh flexibility of the CVD-GM in one of the future prospective works such as pressure-strain, strain-to-electricity and chemical-coupled sensor via I[RBLM] / I[2D] values.

1. Introduction

Graphene, the thinnest as well as the strongest material with two-dimensional layers of hexagonal carbon atoms, have led a lot of researchers and industrial companies to consider its properties and the application in numerous fields. Graphene has attracted tremendous attention in the fields of physical, chemical, electrical and biological sciences since its discovery in 2004 [1–4]. Among various application fields, we now attempt to explore the surface status of graphene monolayer (GM) grown by chemical deposition vapor (CVD) method in terms of assessing electrical performances in association with the capability of useful flexible / transparent electrode and introducing one of the critical elements for bio-sensing performance in near future. In particular, Guo and coworkers have carried out to investigate the use of widespread biomedical applications, ranging from drug/gene delivery, biological sensing and imaging, antibacterial materials, to biocompatible scaffolds for cell culture [5, 6]. Moreover, there is much attention toward the use of graphene for the development of fluorescence resonance energy transfer (FRET) biosensors. FRET involves the transfer of energy from a donor fluorophore to an acceptor fluorophore and is one of the advanced tools available for measuring nanometer-scale distance and changes, both in vivo and in vitro [7]. Throughout these bio-related application fields, one of the most

common critical issues is to fabricate CVD-GM as suspended as possible owing not to provide unwanted perturbation elements such as strong interaction between substrate and CVD-GM during fabrication [8, 9].

Prior to investigating the bio-sensing application, it is essentially worthwhile to explore the original sensing mechanism. Here, we can propose a quantitative surface-enhanced Raman spectroscopic (SERS) metrology for unraveling the status of morphological corrugation (or protrusion) of the CVD-GM located at Au nanoparticle (NP) / CVD-GM / Au TF (Nanoparticle-on Mirror, NPoM) plasmonic junction [10, 13–16]. A new (or enhanced) Radial Breathing Like Mode (RBLM) SERS signal around ~150 cm^{-1} from CVD-GM spaced in NPoM is evidently observed and intensity ratio between out-of-plane (RBLM) and in-plane (2D) phonon modes (I[RBLM] / I[2D]) can be utlized for exploring the degree of morphological corrugation of GM along with z-direction in a quantitative way.

In this work, we unravel that the value of I[RBLM] / I[2D] can be represented as an important value in revealing electrical performances in terms of generating the relationship between the degree of z-directional morphological corrugation status of a CVD-GM spaced in our NPoM and different degree of carrier mobility in lateral direction with the corresponding sheet resistance values [10] or electron-phonon coupling (EPC) along with z-direction on the CVD-GM [11]. Moreover, we can also expect the I[RBLM] / I[2D] values will be utilized with introducing various kinds of *perturbation elecments* as a form of Au NP / *biomaterials* / CVD-GM / Au TF system. In detail, the spaced biomaterials may interact with surrounding environment such as the CVD-GM representatively and the related I[RBLM] / I[2D] values will may be varied upon the strain-based and chemical-coupled bio-interaction (or sensing) between biomaterials and CVD-GM, assuming the CVD-GM shows homogenious z-directional protrusion.

2. Experimental Procedure

Briefly, a roll of Cu foil is inserted into a quartz tube and heated to 1000°C at a low pressure (~3.0×10^{-3} Torr). After reaching 1000°C, the sample is annealed for 20 min. The Cu foil is heat-treated to increase the grain size and gain higher quality graphene films. Graphene growth is then carried out at 1000°C under 500 mTorr at a rate of 50 s.c.c.m. CH_4 (99.999%) for 30 min in our CVD system. Finally, the sample assembly is rapidly cooled from 1000 to 600°C in ~5 min as a first step and to room temperature in ~55 min under low-pressure conditions (~9.0×10^{-4} Torr). The graphene film grown on a copper foil is covered with poly (methylmethacrylate) (PMMA) and floated in a 0.1M ammonium persulfate [$(NH_2)4S_2O_8$] aqueous solution. The PMMA/graphene film is transferred to a 300 nm SiO_2/p^+Si substrate for Raman spectroscopy and to Au thin film (TF) for SERS after all the copper layers are etched away and the film is rinsed in de-ionized water [12]. The correlated AFM-Raman system is employed for simultaneously acquiring topography of transferred graphene and the Raman spectral image with the semi-contact mode. Au TF with a thickness of 10 nm is formed on a cleaned glass substrate by Ar-ion sputtering evaporation. Independent atomic force microscopy (AFM) measurements reveal that the typical root mean square (rms) roughness of the Au TF to be less than 0.2 nm. After the graphene is transferred onto the Au TF, a drop of Au colloidal NP (nominal diameter ≈ 200 nm, BB International) is

applied (~15 μl) onto the CVD-GM / Au TF, and the assembly is rinsed and air-dried at ambient temperature [13].

3. Results And Discussions

Previously, Park and colleagues could explore that the shape of the deposited CVD-GM spaced between Au NP-Cu foil was not always flat and deduced that it might be composed of a partially corrugated CVD-GM as a result of interaction between z-polarized excitation field and the corresponding parallel z-directional phonon mode of CVD-GM, similar to the radial breathing mode (RBM) from single walled carbon nanotubes (SWCNTs). Hence, this specific out-of-plane phonon mode could be identified as RBLM modes [14–16]. In addition, it was also simulated by finite difference time-domain (FDTD) electrodynamics calculation that the origin of RBLM mode could be identified as a result of simple dipole-image-dipole interaction model and it had a pivotal role to generate a z-polarized excitation electromagnetic (EM) field [16]. By virtue of this theoretical result, we can find out the motivation of this work in terms of providing a straightforward nanoscale metrology to quantitatively and optically evaluate the degree of z-directional morphological corrugation of CVD-GM with corresponding electrical properties (lateral carrier mobility or sheet resistance value) and the availability toward biomedical application fields, emphasizing the importance of morphological surface status of CVD-GM, resulting in different values of the I[out-of-plane, RBLM] / I[in-plane, 2D] at certain domain due to probably insertion of biomaterials likewise Au NP / *biomaterials* / CVD-GM / Au TF formation. Figure 1 shows the representative four pairs of SERS spectra of CVD-GM spaced in our NPoM system, highlighting the RBLM (A) and the corresponding 2D peak region (B).

Previously, our plasmonic NPoM system showed a slight increase in the Full Width at Half-Maximum (FWHM) of the 2D peak with corresponding increase of intensity of RBLM signal. At that time, it was still vague to determine the definite relationship between the RBLM intensity and the corresponding local structure [15]. In contrast to the previous report, we can now try to establish a new and more straightforward metrology concept than before. From top to bottom in each Figure 1(A) and (B), we can exhibit four sets SERS spectra of CVD-GM spaced at four different NPoMs [15, 17]. At this time, it is worthwhile to note that the RBLM mode from (A) and 2D mode from (B) can be represented as an out-of-plane and an in-plane phonon mode, respectively, as mentioned earlier. Therefore, the intensity ratio between out-of-plane and in-plane phonon mode likewise I[RBLM] / I[2D] maybe one of the meaningful and straightforward value beyond optical diffraction to limit to quantitatively estimate among the degree of z-directional morphological corrugation status, the corresponding lateral carrier mobility and bio-medical application fields utilizing of high specific surface area and ultrahigh flexibility of a CVD-GM surface, leading to variable I[RBLM] / I[2D] values depending on the degree of pressure-strain, strain-to-electricity and chemical-coupled interaction with the very surrounded CVD-GM [18].

Table 1
(I[RBLM] / I[2D] values at each NPoM)

Number of NPoM	I[RBLM] / I[2D]
#1	1.67
#2	1.61
#3	1.33
#4	0.75

Table 1 shows the calculated I[RBLM] / I[2D] values at each NPoM system. As we anticipated, the significant difference values are clearly observed, indicating that the degree of z-directional morphological corrugation of CVD-GM from #1 NPoM case exhibits the highest among these four sets. Hence, we can quantitatively assess the degree of z-directional morphological corrugation of CVD-GM domains as follows #1 > #2 > #3 > #4, shown below in Figure 2.

Moreover, we can also readily anticipate that higher I[RBLM] / I[2D] value indicates the lower lateral carrier mobility (or higher sheet resistance value) due to different CVD-GM shape, especially, along z-direction (ex: mountain or plain), which could be expressed as the relationship between Raman 2D peak maximum position of the CVD-GM and the corresponding electrostatic force microscope (EFM) results [19, 20]. In detail, the compressive strain effect (relatively blue-shift of a 2D peak maximum position) was investigated in relatively complex and surrounded CVD-GM ripple domains with lower amplitude voltages, indicating more charged domains through the EFM experiment while relatively higher EFM amplitude voltage was observed in threading (or relatively non-complex) CVD-GM ripple domains, explaining less charged domains. At that time, the local structure revealed by AFM topography could be employed in estimating the correlation study between optical Raman microscopy results regarding the strain effect as well as the degree of surface charge effect revealed by EFM (Please see the Figure S1 in supplementary material).

Overall, a relatively higher surface charged domain obtained via higher EFM amplitude imaging technique is in sync with a relatively higher and complex domains as a result of an AFM topography or the degree of the correlated blue-shifted Raman in-plane (G or 2D) maximum peak position [8, 19, 20]. Moreover, the relationship between higher degree of blue-shifted Raman in-plane (G or 2D) maximum peak positions and the resultant higher degree of sheet resistance (lower lateral carrier mobility) values was clearly substantiated in this work [8].

Furthermore, it is undergoing to establish the correlation between I[RBLM] / I[2D] and real root mean square (rms) roughness by atomic force microscope (AFM) measurement for the purpose of precisely correlating with I[RBLM] / I[2D] obtained via optical Raman microscopy. Once we establish the correlation

between I[RBLM] / I[2D] and rms roughness using the AFM system, we may not have some complexities such as elaborate operation and many times of replacement of expensive AFM tips.

Figure 3(A) describes schematic relationship between relatively higher and lower degree of z-directional structure of the CVD-GM. It gives us an important meaning the 3(A) shows relatively less lateral carrier mobility due to higher degree of z-protrusion, whereas 3(B) deciphers relatively lower degree of z-directional structure of CVD-GM, indicating higher lateral carrier mobility. Accordingly, we can now readily understand that the higher value of I[RBLM] / I[2D] is corresponding with Figure 3(A), whereas the lower value of I[RBLM] / I[2D] is corresponding with Figure 3(B). Furthermore, the simultaneous observation of a sequential blue-shift of the RBLM peak from bottom to top in Figure 1(A) may exhibit that a degree of n-doping caused by a high electron phonon coupling (EPC) along z-direction at the Au NP / CVD-GM / Au TF may be observed and we can claim that the degree of EPC and n-doping can be ascribed to the relatively high degree of z-polarized EM and resultant higher contribution of out-of-plane phonon movement in our NPoM systems [21].

4. Conclusion

To conclude, we can quantitatively suggest a spectroscopic indicator revealing the status of z-directional morphological corrugation of a CVD-GM after transfer onto the Au thin film. By applying Nanoparticle-on-Mirror (NPoM) system composed of Au NP / CVD-GM / Au TF, a new (or enhanced) Radial Breathing Like Mode (RBLM) SERS signal around ~150 cm^{-1} from a spaced CVD-GM is clearly observed by employing a local z-polarized incident field formed at the Au NP–Au TF plasmonic junction. Accordingly, the correlation study using I[RBLM] / I[2D] value can suggest a new optical nano-metrology tool to determine the degree of morphological corrugation status of a CVD-GM, resulting in as a simple optical tool for estimating relative electrical performance such as lateral carrier mobility, sheet resistance value and surface charge disyribution upon local morphology of a CVD-GM. Furthermore, the CVD-GM will be excellent bio-medical application platform in consideration of the high specific or largely homogeneous surface area and ultrahigh flexibility for bio-sensing such as the different degree of pressure-strain, chemical-coupling sensing as a Au NP/ biomaterials / CVD-GM / Au TF system with systematic change of I[RBLM] / I[2D] value.

Declarations

Acknowledgement / Funding

This research was funded by the Basic Science Research Program through the National Research Foundation of Korea (NRF) funded by the Ministry of Education (2021R1I1A1A01058271).

Authors' contributions

The author carried out all tasks associated to the elaboration of the manuscript: conception, design, result analysis, and writing.

Availability of data and material

The datasets generated during and/or analyzed during the current study are available from the corresponding author on reasonable request.

Code availability (software application or custom code)

The datasets generated during and/or analyzed during the current study are available from the corresponding author on reasonable request.

Conflicts of Interests

The author declares no conflict of interest.

Consent to Participate

Not applicable

Consent of Publication

Not applicable

Ethics approval

Not applicable

References

1. Geim AK, Novoselov KS (2007) The rise of graphene. Nat Mater 6:183–191
2. Geim AK (2009) Graphene: Status and Prospects. Science 19:1530–1534
3. Zou X, Wei S, Jasensky J, Xiao M, Wang, Brooks CL, Chen Z (2017) Molecular Interactions between Graphene and Biological Molecules. J Am Chem Soc 139:1928–1936
4. Chung C, Kim Y-K, Shin D, Ryoo S-R, Hong BH, Min D-H (2013) Biomedical Applications of Graphene and Graphene Oxide. Acc Chem Res 46:2211–2224
5. Guo S, Dong S (2011) Graphenenanosheet: synthesis, molecular engineering, thin film, hybrids, and energy and analytical applications. Chem Soc Rev 40:2644–2672
6. Jiang H-J (2011) Chemical Preparation of Graphene-Based Nanomaterials and Their Applications in Chemical and Biological Sensors. small 17:2413–2427
7. Selvin PR (2000) The renaissance of fluorescence resonance energy transfer. Nat Struct Biol 7:730–734
8. Park W-H (2014) Electrical performance of chemical vapor deposition graphene on PET substrate tailored by Cu foil surface morphology. Eur Phys J Appl Phys 67:30701

9. Park W-H, Jung M, Moon J-S, Park W, Kim T, Lee J, Joo M, Park K (2013) Experimental observation of a suspended single layer graphene film on Cu foil grown via chemical vapor deposition method. Phys Status Solidi B 250:1874–1877
10. Deng S, Berry V (2016) Wrinkled, rippled and crumpled graphene: an overview of formation mechanism, electronic properties, and applications. Mater Today 19:197–212
11. Park W-H, Cheong H (2016) Exploring the SERS background using a sandwiched graphene monolayer with gap-plasmon junctions. J Phys D: Appl Phys 49:105302
12. Jo I, Kim Y, Moon J, Park S, Moon J-S, Park W, Lee JS, Hong BH (2015) Stable n-type doping of graphene via high-molecular-weight ethylene amines. Phys Chem Chem Phys 17:29492–29495
13. Park W-H, Ahn S-H, Kim ZH (2008) Surface-Enhanced Raman Scattering from a Single Nanoparticle–Plane Junction. ChemPhysChem 9:2491–2494
14. Park W-H, Jung M (2016) Out-of-Plane Directional Charge Transfer-Assisted Chemical Enhancement in the Surface-Enhanced Raman Spectroscopy of a Graphene Monolayer. J Phys Chem C 120:24354–24359
15. Min YH, Park W-H (2014) Exploring the relative bending of a CVD graphene monolayer with gap-plasmons. Nanoscale 6:9763–9766
16. Ahn S-H, Park W-H, Kim ZH (2007) Nano-Optical Investigation of Enhanced Field at Gold Nanosphere-Gold Plane Junctions. Bull Korean Chem Soc 28:2200–2202
17. Benz F, Chikkaraddy R, Salmon A, Ohadi H, de Nijs B, Mertens J, Carnegie C, Bowman RW, Baumberg JJ (2016) SERS of Individual Nanoparticles on a Mirror: Size Does Matter, but so Does Shape. J Phys Chem Lett 7:2264–2269
18. Eissa S, Jimenez GC, Mahvash F, Guermoune A, Tlili C, Szkopek T, Zourob M, Siaj M (2015) Functionalized CVD Monolayer Graphene for Label-Free Impedimetric Biosensing. Nano Res 8:1698–1709
19. Park W-H *Nanomaterials*. (2021) Nano-Physical Characterization of Chemical Vapor Deposition-Grown Monolayer Graphene for High Performance Electrode: Raman, Surface-Enhanced Raman Spectroscopy, and Electrostatic Force Microscopy Studies. 11: 2839
20. Park W-H, Kim M, Choo J, Cheong H (2018) Experimental investigation of surface morphology of a chemical vapor deposition-grown graphene monolayer mediating with a gap-plasmonic system and the related ripple shape study. J Appl Phys 124:223101
21. Park W-H (2014) Quantification of the Relative z-Polarized Electromagnetic Field Contribution and Associated Investigation of Asymmetric Shape of Layer Breathing Mode from Au Nanoparticle–Graphene–Au Thin Film Junctions. J Phys Chem C 118:6989–6993

Figures

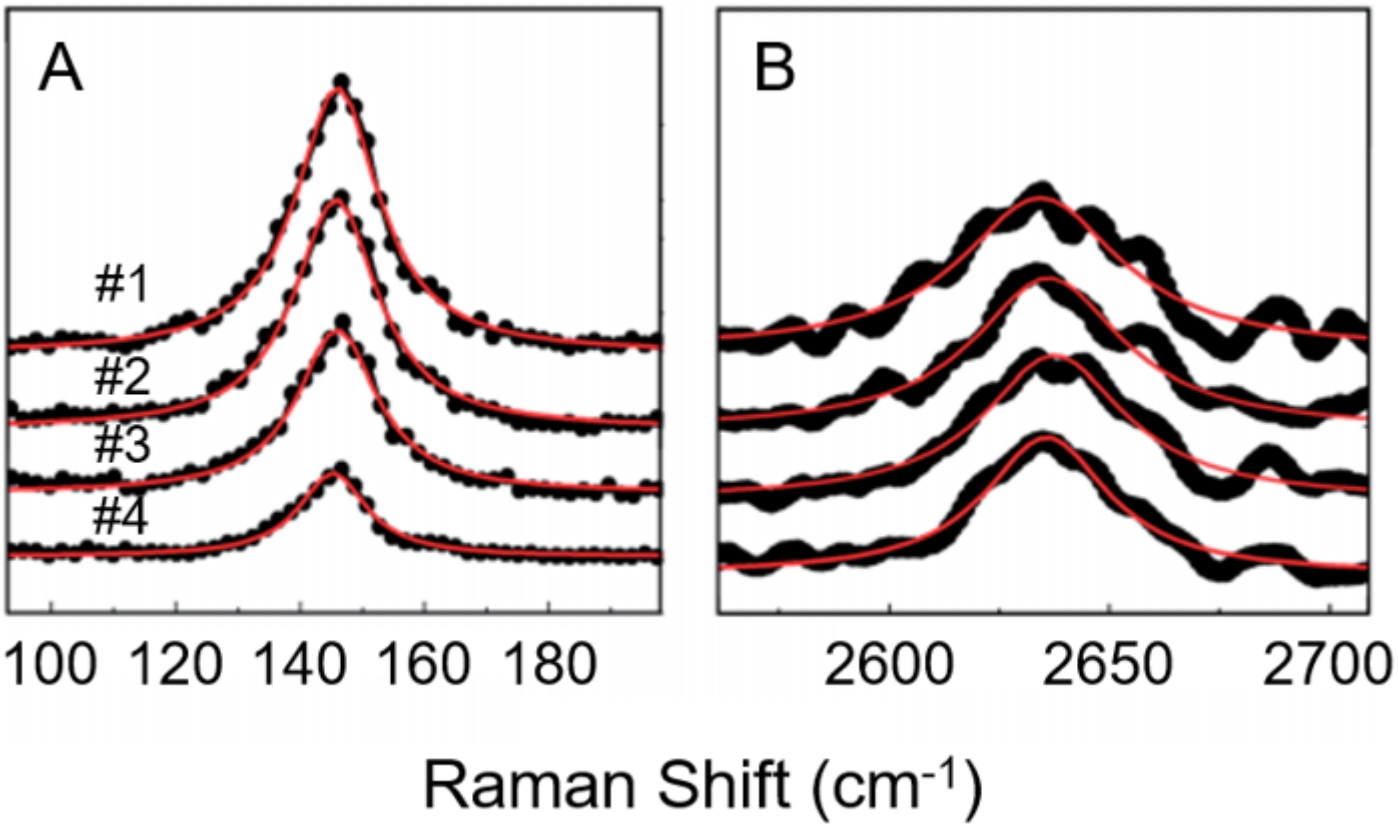

Figure 1

Representative four sets of SERS spectra. (A) presents newly observed 4 RBLM peaks at ~ 150 cm^{-1} and (B) exhibits the corresponding 2D peaks. The top spectra at each (A) and (B) are obtained at the same NPoM plasmonic junction and the rests of the subsequent numbered spectra are also obtained at the same NPoM plasmonic junctions [15].

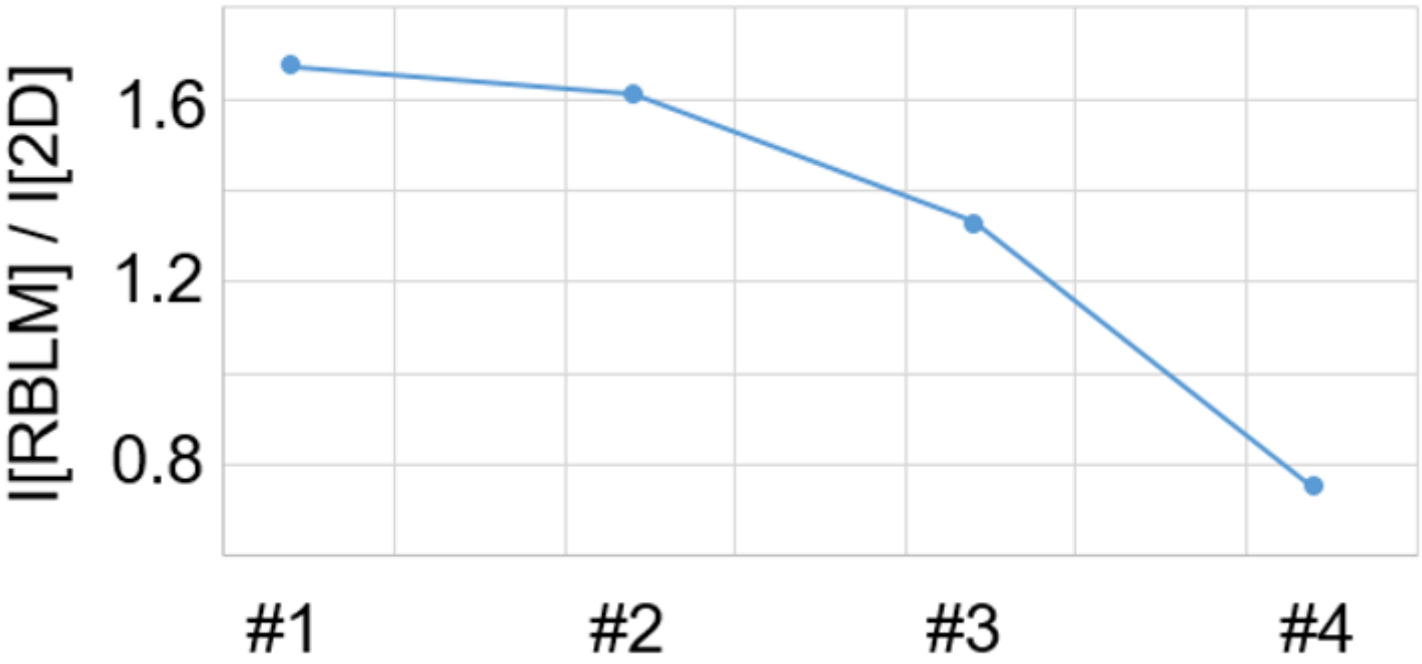

Figure 2

The graph shows the four sets of I[RBLM] / I[2D] values at each NPoM.

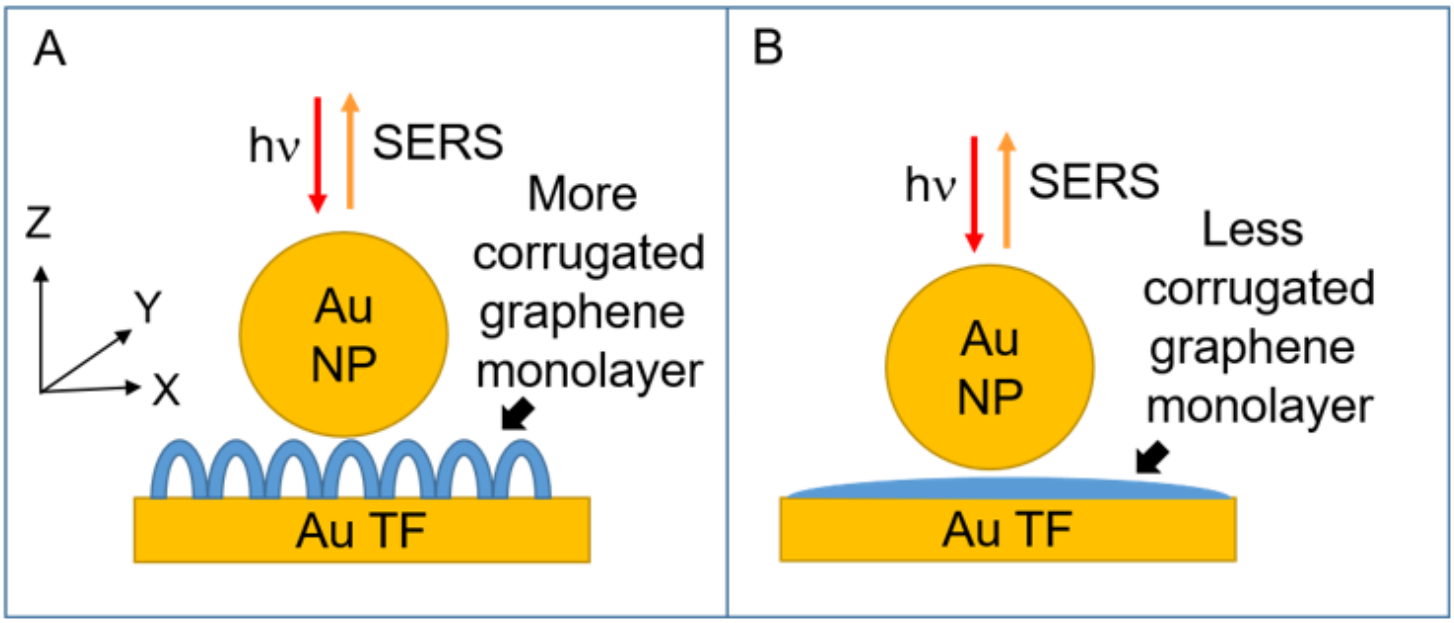

Figure 3

(A) and (B) show schematic pictures deciphering the plausible formations of the spaced CVD-GM in our NPoM structures. (A) and (B) are relatively more corrugated (less lateral carrier mobility) and less corrugated (more lateral carrier mobility) CVD-GM along with z-direction, respectively.

Supplementary Files

This is a list of supplementary files associated with this preprint. Click to download.

- SupplementryMaterial.docx